

# Local spin relaxation within the random Heisenberg chain

J. Herbrych<sup>1</sup>, J. Kokalj<sup>1</sup>, and P. Prelovšek<sup>1,2</sup>

<sup>1</sup>*J. Stefan Institute, SI-1000 Ljubljana, Slovenia and*

<sup>2</sup>*Faculty of Mathematics and Physics, University of Ljubljana, SI-1000 Ljubljana, Slovenia*

(Dated: December 3, 2024)

Finite-temperature local spin dynamics within the random spin-1/2 antiferromagnetic Heisenberg chain is studied numerically. The aim is to explain measured NMR spin-lattice relaxation times in  $\text{BaCu}_2(\text{Si}_{0.5}\text{Ge}_{0.5})_2\text{O}_7$ , which is the realization of a random spin chain. In agreement with experiments we find that the distribution of relaxation times within the model shows a very large span similar to the stretched-exponential form. The distribution is strongly reduced with increasing  $T$ , but stays finite also in the high- $T$  limit. Our results reveal the crucial role of the anisotropy (interaction), since the behavior is essentially contrast with the ones for XX model (equivalent to noninteracting fermions), where we do not find any significant  $T$  dependence of the distribution.

PACS numbers: 05.60.Gg, 71.27.+a, 75.10.Pq, 76.60.-k

One-dimensional (1D) quantum spin systems with random exchange couplings reveal interesting phenomena fundamentally different from the behavior of ordered chains. Since the seminal studies of antiferromagnetic (AFM) random Heisenberg chains (RHC) by Dasgupta and Ma [1, 2] using the renormalization-group approach and further development by Fisher [3], it has been recognized that the quenched disorder of exchange couplings  $J$  leads at lowest energies to the formation of random singlets with vanishing effective  $\tilde{J}$  at large distances. The consequence for the static susceptibility  $\chi^0$  is the singular Curie-type temperature  $T$  dependence, dominated by nearly uncoupled spins at low- $T$  and confirmed by numerical studies of model systems [4], as well by measurements of  $\chi^0(T)$  on the class of materials being the realizations of RHC physics, in particular the mixed system  $\text{BaCu}_2(\text{Si}_{1-x}\text{Ge}_x)_2\text{O}_7$  [5–7].

Much less is understood about the dynamical properties of RHC systems. This has become evident in connection with the recent measurements of NMR spin-lattice relaxation times  $T_1$  in  $\text{BaCu}_2(\text{Si}_{0.5}\text{Ge}_{0.5})_2\text{O}_7$  [6], which reveal a broad distribution of different  $T_1$  resulting in a nonexponential magnetisation decay being rather of a stretched-exponential form. In this connection the most remarkable is the strong  $T$  dependence of the  $T_1$  span becoming progressively large and the corresponding distribution non-Gaussian at low- $T$ . It is evident that in a random system  $T_1$ , which is predominantly testing the local spin correlation function  $S_{nn}(\omega \rightarrow 0)$ , becomes site  $n$  dependent and we are therefore dealing with the distribution of  $T_{1n}$  leading to a nonexponential magnetisation decay.

Theoretically the behavior of dynamical spin correlations in RHC, in particular their  $T$  dependence, is not understood and has not been adequately addressed so far. It seems plausible that the low- $T$  behavior should follow from the random-singlet concept and its scaling properties, discussed within the framework of the renormalization-group approaches [2, 3, 8, 9]. In this respect one open question is also the qualitative similarity to the behavior of the random anisotropic XX chain invoked in several studies [4, 8–10]. The latter system is equivalent to more elaborated problem of noninteracting (NI) spinless fermions with the off-diagonal

(hopping) disorder [11, 12]. In the latter case, it is well established that single-particle functions are localized except in the middle of the band and the latter anomaly is reflected in the singular single-particle density of states (DOS).

In the following we present results for the dynamical local spin correlation function  $S_{nn}(\omega)$ , in particular for its d.c. limit  $s = S_{nn}(\omega \rightarrow 0)$  relevant for the NMR  $T_1$ , within the AFM RHC model for  $T > 0$ , obtained using the numerical method based on the density-matrix renormalization group (DMRG) approach [13]. At high  $T \geq J$ , distribution of  $s$  can be approached even analytically via moment expansion and reveals a modest but finite width qualitatively similar both for the isotropic and the XX chain. On the other hand, the  $T$  variation established numerically is essentially different. While for the XX chain there is no significant  $T$  dependence, results for the isotropic case reveal at low  $T \ll J$  a very large span of  $s$  values and corresponding  $T_{1n}$ , qualitatively and even quantitatively consistent with NMR experiments [6].

We study in the following the one-dimensional spin-1/2 model representing the AFM RHC,

$$H = \sum_i J_i (S_i^x S_{i+1}^x + S_i^y S_{i+1}^y + \Delta S_i^z S_{i+1}^z), \quad (1)$$

where  $J_i$  are random and we will assume their distribution as uncorrelated and uniform in the interval  $J - \delta J \leq J_i \leq J + \delta J$ , with the width  $\delta J < J$  as the parameter. In the following we will consider predominantly the isotropic case  $\Delta = 1$  but as well the anisotropic XX case with  $\Delta = 0$ . The chain is of the length  $L$  with open boundary conditions (o.b.c.) as useful for the DMRG method. We further on use  $J = 1$  as the unit of energy as well as  $\hbar = k_B = 1$ .

Our aim is to analyse the local spin dynamics in connection with the NMR spin-lattice relaxation [6]. In a homogeneous system the corresponding relaxation rate  $1/T_1$  is expressed in terms of the  $q$ -dependent spin correlation function,

$$\frac{1}{T_1} = \sum_{q\alpha} A_\alpha^2(q) S^{\alpha\alpha}(q, \omega \rightarrow 0), \quad (2)$$

where  $A_\alpha^2(q)$  involve hyperfine interactions and NMR form factors [6]. Since the dominant contribution in an AFM chain

at low- $T$  is coming from the regime  $q \sim \pi$  [14] (we comment on possible role of  $q \rightarrow 0$  contribution in the summary) the variation  $A_\alpha^2(q)$  is not essential and the rate depends only on the local spin correlation function  $1/T_1 \propto S_{\text{loc}}^{zz}(\omega \rightarrow 0)$ . In a system with quenched disorder the relaxation time becomes site dependent, i.e.  $T_{1n}$ , hence we study in the following the local correlations  $S_{nn}(\omega)$  and the distribution of local d.c. limits  $s = S_{nn}(\omega \rightarrow 0)$  and related relaxation times  $\tau = 1/s$  where

$$S_{nn}(\omega) = \frac{1}{\pi} \text{Re} \int_0^\infty dt e^{i\omega t} \langle S_n^z(t) S_n^z(0) \rangle. \quad (3)$$

Numerically we focus on the most interesting  $T < J$  regime. In order to reduce finite-size effects we study large systems employing the finite-temperature dynamical DMRG (FTD-DMRG) [13, 15] method to evaluate the dynamical  $S_{nn}(\omega)$ , Eq. (3). The approach is based on the DMRG optimization of basis states [16, 17], combined with the finite-temperature Lanczos method (FTLM) [18] and recently used to study  $T > 0$  dynamical spin correlations within  $J_1$ - $J_2$  model [19]. To reduce edge effects we choose the local site  $n$  to be in the middle of the chain,  $n = L/2$ . The distribution of  $s$  is then calculated with  $N_r \sim 10^3$  different realizations of random  $J_i$ . These are introduced at the beginning of the *finite*-DMRG procedure, while the *infinite* part of DMRG is performed for a homogeneous  $J_i = J$  system [20]. With  $M \sim 200$  basis states kept per DMRG block one can deal with  $L = 80$  for  $T < J/2$  without considerable truncation error. More elevated  $T > J/2$  would require larger  $M$ , but due to reduced finite-size effects smaller systems  $L \sim 20$  are enough where full basis can be kept. Also, the randomness of  $J_i$  and related tendency towards local singlets or triples further reduces the entanglement making the method more suitable for studying random systems. More technical detail on the calculation can be found in the Supplement [20].

We start the presentation of results with typical examples of  $S_{nn}(\omega)$ . In Fig. 1 we show calculated spectra for system with  $L = 80$  sites,  $T = 0.5$ ,  $\Delta = 1$ , and three different realizations of  $J_i$ , i.e. the homogeneous system with  $J_i = 1$  and two configurations with  $\delta J = 0.5$ . The broadening  $\delta = 0.05$  is used in the presentation of  $S_{nn}(\omega)$ . Spectra for the uniform system are broad and regular at  $\omega \sim 0$  agreeing with those obtained with other methods [21], while  $S_{nn}(\omega)$  for random case strongly depend apart from  $\delta J$  also on the local  $J_i$ ,  $i \sim n$ . In particular, spectra with both  $J_n$  and  $J_{n-1}$  small have large amplitude at the relevant  $\omega \sim 0$ , while spectra with one large  $J_n$  or  $J_{n-1}$  have most of the weight at high- $\omega$  and small amplitude at  $\omega \sim 0$  (elaborated further in the conclusions). For the following analysis it is important that  $s = S_{nn}(\omega \rightarrow 0)$  can be extracted reliably. We also note that the sum rule  $\int d\omega S_{nn}(\omega) = 1/4$  is  $T$  and configuration independent.

**Results for  $T \geq J$ :** Before displaying results for most interesting  $T < J$  regime, we note that even at  $T \gg J$  one cannot expect a well defined  $\tau = \tau_0$  but rather a distribution of values. One can understand this by studying local fre-

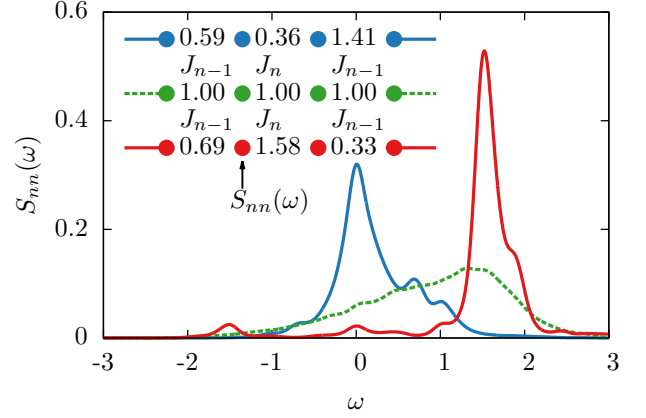


Figure 1. (Color online) Dynamical local spin correlations  $S_{nn}(\omega)$  for different configurations of  $J_i$ . Shown are spectra for the homogeneous case  $\delta J = 0$  and two configurations with  $\delta J = 0.5$ , calculated for  $T = 0.5$  and  $L = 80$  sites. Note that  $S_{nn}(\omega)$  for sites with weak (strong) neighboring bonds has large contribution at small (large)  $\omega$ .

quency moments  $m_{ln} = \int d\omega \omega^l S_{nn}(\omega)$ . The latter can be evaluated analytically within the high- $T$  expansion for given site  $n$  and each particular configuration  $J_i$ . Expressions for  $T \rightarrow \infty$  are given in the Supplement [20] and clearly depend only on the  $J_i$ ,  $i \sim n$ , with an increasing number of neighbors involved for larger  $l$  ( $m_{ln} = 0$  for odd  $l$  for  $T \rightarrow \infty$ ). Using then the Mori's continued fraction representation [22] and the Gaussian-type truncation at the level of  $l > 3$  [23, 24] we get explicit  $S_{nn}(\omega)$  (given in the Supplement) as well as  $s$  involving  $J_i$ ,  $i = n-2, \dots, n+1$ . It is then straightforward to calculate the probability distribution function (PDF) for  $s$ . In Fig. 2 we present high- $T$  result for PDF( $s$ ) obtained from the moment expansion and compared with the numerical results evaluated for  $T = 1$ ,  $L = 20$  with full basis and averaged over  $N_r = 10^3$  realizations. Several conclusions can be drawn from presented results: (a) The agreement of PDF( $s$ ) obtained via the analytical approach and fully numerical FTD-DMRG method is satisfactory having the origin in quite broad and featureless spectra  $S_{nn}(\omega)$  at  $T \geq J$ . Still we note that median value of  $s$  ( $s_{\text{med}}$ ) differ between both approaches (less than factor of 2) and that for  $T \gg J$  (unlike  $T \sim J$ ) contribution of  $q \rightarrow 0$  can become essential [25]. (b) PDF( $s$ ) becomes quite asymmetric and broad for  $\delta J \geq 0.5$ . (c) Consequently, also the distribution of local relaxation times PDF( $\tau$ ) has finite but modest width for  $T \rightarrow \infty$ . This seems in a qualitative agreement with NMR data for  $\text{BaCu}_2(\text{Si}_{0.5}\text{Ge}_{0.5})_2\text{O}_7$  (with effective randomness  $\delta J \simeq 0.35$ ), where the width was hardly detected in the high- $T$  limit [6].

**Results for  $T < J$ :** More challenging is the low- $T$  regime which we study using the FTD-DMRG method for typically  $L = 80$  and  $N_r \sim 10^3$ . Besides the isotropic case ( $\Delta = 1$ ), we investigate for comparison also the XX model ( $\Delta = 0$ ). As the model of NI fermions with the off-diagonal disorder [10, 11] it can be easily studied via full diagonalization on much longer chains with  $L \sim 16000$ . PDF for  $T < J$

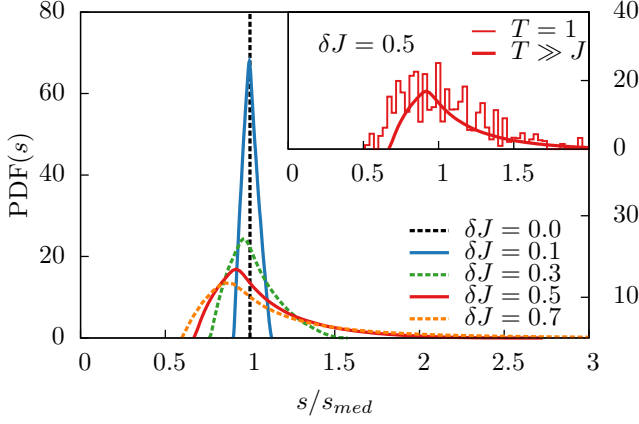


Figure 2. (Color online) Probability distribution function of local relaxation rates  $\text{PDF}(s)$  at  $T \gg J$  evaluated using the moment expansion for different  $\delta J$ . Inset: Comparison of analytical and FTD-DMRG result for  $\delta J = 0.5$ .

can become very broad and asymmetric. Hence, we rather present results as the cumulative distribution  $\text{CDF}(x) = \int_0^x dy \text{PDF}(y)$ . Further we rescale  $x$  values to the median defined as  $\text{CDF}(x_{\text{med}}) = 0.5$ . Results for  $\text{CDF}(s)$  as well as  $\text{CDF}(\tau)$  are presented in Fig. 3. Note that both PDF are related as  $\text{PDF}(\tau) = \text{PDF}(s)/\tau^2$ . First two panels in Fig. 3 represent results for the isotropic case  $\Delta = 1$  with (a) fixed  $T = 0.2$  and varying  $\delta J = 0.1 - 0.9$ , while in (b)  $\delta J = 0.7$  is fixed and  $T = 0.1 - 0.5$ . Fig. 3c displays the  $T$  dependence of CDF for the  $\Delta = 0$  case.

We first note that within the XX chain  $\text{CDF}(s)$  are essentially  $T$  independent. This appears as quite a contrast to, e.g., static  $\chi^0(T)$  which exhibits a divergence at  $T \rightarrow 0$  [4, 20]. Results for the isotropic case  $\Delta = 1$  in Figs. 3a,b are evidently different. The span in CDF becomes very large (note the logarithmic scale) either by increasing  $\delta J$  at fixed  $T$  or even more by decreasing  $T$  at fixed  $\delta J$ . From the corresponding PDF one can calculate the relaxation function  $R(t) = \int ds \text{PDF}(s)e^{-ts}$ , which is in fact the quantity directly measured in the NMR as a time-dependent magnetisation recovery [6]. As in experiment the large span in our results for low- $T$  can be well captured by a stretched exponential form,

$$R(t) \approx \exp \left[ - (t/\tau_0)^\Gamma \right], \quad (4)$$

where  $\Gamma$  and  $\tau_0$  are parameters to be fitted for particular  $\text{PDF}(s)$ . It is evident that  $\Gamma \ll 1$  means large deviations from the Gaussian-like form, and in particular very pronounced tails in  $\text{PDF}(s)$ , both for  $s \gg s_{\text{med}}$  as well as a singular variation for  $s \rightarrow 0$ . In the latter regime  $1/\tau_0$  can deviate substantially from average of local  $1/\tau$ . It should be also noted that the form, Eq. (4), is the simplest one capturing the large span of  $s$  values. It is also used in the experimental analysis [6], but the corresponding  $\text{PDF}(s)$  reveal somewhat enhanced tails for  $s > s_{\text{med}}$  relative to calculated ones in Fig. 3a,b, and

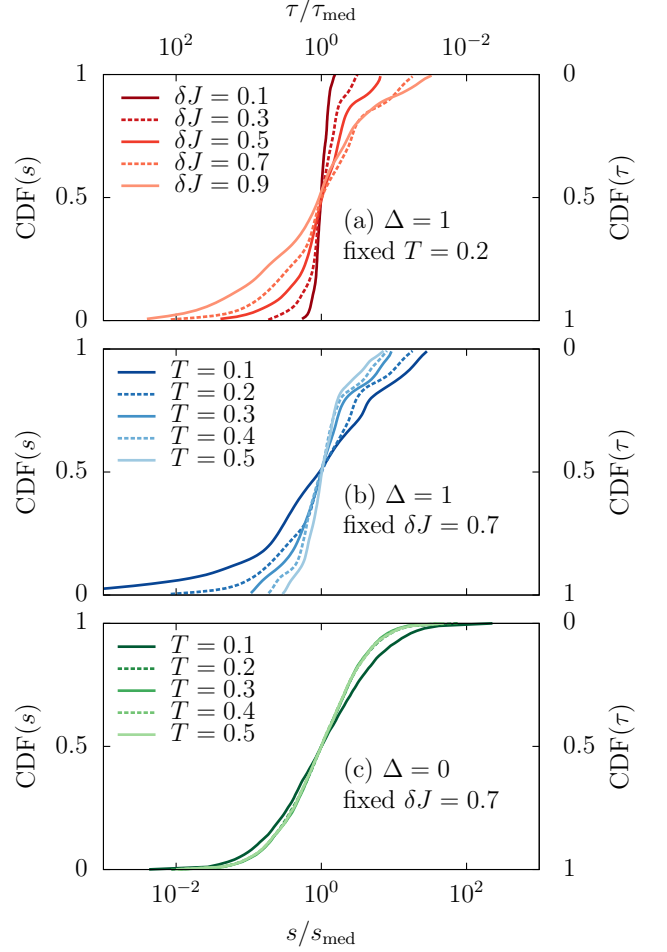


Figure 3. (Color online) Cumulative distribution function of  $s$  and  $\tau = 1/s$ . Shown are FTD-DMRG results for  $\Delta = 1$ : (a) for fixed  $T = 0.2$  and various  $\delta J$ , (b) for fixed  $\delta J = 0.7$  and various  $T \leq 0.5$ , and (c) full diagonalization results for  $\Delta = 0$ ,  $\delta J = 0.7$  and various  $T$ .

the opposite trend for  $s < s_{\text{med}}$ .

Results for the fitted exponent  $\Gamma(T)$  for  $\Delta = 1$  as extracted from numerical  $\text{PDF}(s)$  for various  $\delta J$  are shown in Fig. 4a. They confirm experimental observation [6] of increasing deviations from simple exponential variation ( $\Gamma = 1$ ) for  $T \ll J$ . While for  $T > J$ ,  $\Gamma \lesssim 1$  for modest  $\delta J < 0.7$ , low- $T$  values can reach even  $\Gamma < 0.5$  at lowest reachable  $T < 0.1$ . Note that in such a case values of  $s$  are distributed over several orders of magnitude.

Of interest for the comparison with experiment is also the  $T$  variation of fitted  $1/\tau_0$ . Results are again essentially different for  $\Delta = 0$  and  $\Delta = 1$ .  $\tau_0$  (as well  $s_{\text{med}}$ ) for  $\Delta = 0$  follows well the Korringa law  $1/\tau_0 \propto T$  for  $T < 0.5$ , as usual for the system of NI fermions with a constant DOS (divergent DOS at  $E \rightarrow 0$  could induce a logarithmic correction). On the other hand, for the isotropic  $\Delta = 1$  pure chain with no randomness  $\tau_0 = \tau$  it should follow  $1/\tau \sim \text{const.}$  for  $T < J$  [14, 21]. Similar behavior is observed for weak disorder  $\delta J = 0.1$  as

shown in Fig. 4b. However, with increasing randomness  $\delta J$ ,  $1/\tau_0$  becomes more  $T$  dependent and increases with  $T$ .

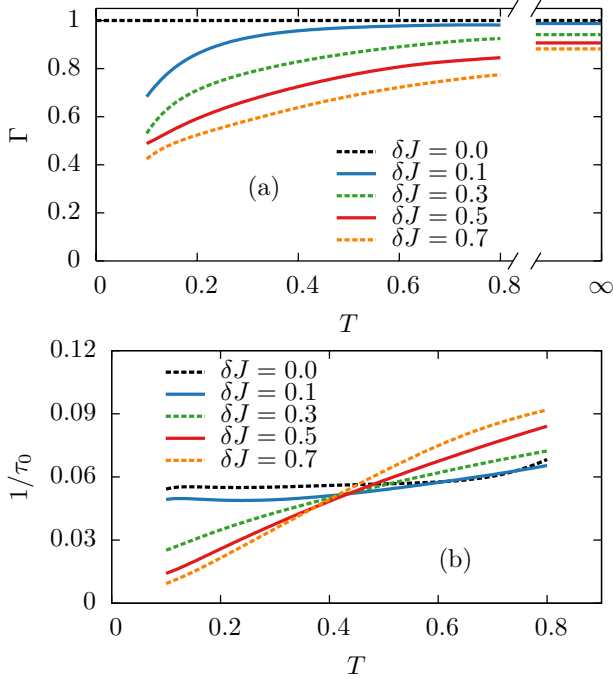


Figure 4. (Color online) (a) Exponent  $\Gamma$  vs.  $T$  obtained from  $\text{PDF}(s)$  data for different  $\delta J$  and isotropic case  $\Delta = 1$ . (b)  $T$  dependence of fitted  $1/\tau_0$  for  $\Delta = 1$  and different  $\delta J$ .

As a partial summary of our results, we comment on the relation to the experiment on  $\text{BaCu}_2(\text{Si}_{0.5}\text{Ge}_{0.5})_2\text{O}_7$ . The spin chain is in this case assumed to be random mixture of two different values  $J_i = 280$  K, 580 K, which correspond roughly to our  $\delta J = 0.35$  (fixing the same effective width) and  $J = 430$  K. Taking these values, our results for  $\Gamma(T)$  as well as  $1/\tau_0(T)$  agree well with experiment reported in Ref. [6]. In particular we note that at lowest  $T \ll J$  our calculated  $\Gamma \sim 0.5$  for  $\delta J = 0.3$  matches the measured one. Some discrepancy appears to be a steeper increase of measured  $\Gamma(T)$  towards the limiting  $\Gamma = 1$  coinciding with observed very narrow  $\text{PDF}(\tau)$  which remains of finite width in our results even for  $T \rightarrow \infty$  as seen in Fig. 2. As far as calculated  $1/\tau_0(T)$  vs. NMR experiment is concerned we note that taken into account the normalization of average  $J$  at low  $T \rightarrow 0$  disordered system reveals smaller  $1/\tau_0$  than a pure one consistent with the experiment [6]. In agreement with the experimental analysis is also strong  $T$  variation of  $1/\tau_0$  in disordered system in contrast to a pure one.

Our results on the local spin relaxation  $S_{nn}(\omega)$  and in particular its  $T$  dependence cannot be directly explained within the framework of existing theoretical studies and scaling approaches to RHC [2, 3, 9]. Our study clearly shows the qualitative difference in the behavior of the XX chain and the isotropic RHC. While in the former model mapped on NI electrons  $T$  does not play any significant role on  $\text{PDF}(s)$  as seen

in Fig. 3c,  $\Delta = 1$  case shows strong variation with  $T \ll J$ . It is plausible that the difference comes from the interaction and many-body character involved in the isotropic RHC. To account for that we design in the following a simple qualitative argument.

The behavior of  $S_{nn}(\omega \sim 0)$  at low- $T$  is dominated by transitions between low-lying singlet and triplet states which become in a RHC nearly degenerate following the scaling arguments with effective coupling  $\tilde{J} \rightarrow 0$  for more distant spins and reflected in diverging  $\chi^0(T \rightarrow 0)$  [2–4, 20]. Such transitions are relevant at  $\omega \rightarrow 0$  behavior as presented in Fig. 1. Moreover, local  $S_{nn}(\omega \sim 0)$  exhibit large spread due to the variations in the local environment. Let us for simplicity consider the symmetric Heisenberg model on four sites (with o.b.c.) with a stronger central bond  $J_2 \gg J_1 = J_3$  and  $J = (J_1 + J_2 + J_3)/3$ . It is then straightforward to show that the lowest singlet-triplet splitting is strongly reduced, i.e.  $\Delta E \propto \eta^2 J$  where  $\eta = J_1/J_2$ . Within the same model one can evaluate also the ratio between two different amplitudes of  $S_{nn}(\omega \sim \Delta E) = A_{nn}\delta(\omega - \Delta E)$ , on sites  $n = 1, 2$  neighboring the weak and strong bond,

$$\frac{1}{W} = \frac{A_{22}}{A_{11}} = \frac{|\langle \Psi_t | S_2^z | \Psi_s \rangle|^2}{|\langle \Psi_t | S_1^z | \Psi_s \rangle|^2} \sim \eta^2. \quad (5)$$

The relation shows that the span between largest and smallest amplitudes increases as  $W \propto 1/\eta^2 \propto 1/\Delta E$ . Continuing in the same manner the scaling procedure for AFM RHC [2, 3] for a long chain the smallest effective coupling between further spins  $\tilde{J}$  vanishes at  $T = 0$  and  $\Delta E \propto \tilde{J} \rightarrow 0$ , so that one expects  $W \rightarrow \infty$  for  $T \rightarrow 0$ . On the other hand, for  $T > 0$  the scaling should be cut off at  $\tilde{J} \sim T$  at least for  $\Delta = 1$ , finally leading to the strong  $W(T)$  dependence ( $W \propto 1/T$ ).

So far, our analysis of local  $s$  was based on assumption that there is no singular contribution emerging from long-wavelength  $q \rightarrow 0$  physics. Indeed, all our available data for  $S^{zz}(q, \omega \rightarrow 0)$  for AFM RHC (not presented) confirm that the dominant regime at low- $T$  is  $q \sim \pi$ . Still,  $q \rightarrow 0$  regime needs further attention since it can lead at  $T > J$  to a divergent  $S_{nn}(\omega \rightarrow 0) \propto 1/\omega^\alpha$  either from the propagation (prevented by randomness in the RHC) in the homogeneous XX chain [21] (with  $\alpha \rightarrow 0$ ) or even more as the consequence of the spin diffusion [26] ( $\alpha = 1/2$ ). The latter can be realized at  $T > 0$  but vanishes at  $T \rightarrow 0$  within the RHC [9, 11]. Our results so far indicate that in spite of possible  $T > 0$  diffusion its contribution to  $S_{nn}(\omega \rightarrow 0)$  is unresolvable for reachable systems, as follows also from NMR experiments [6] where it can be directly tested via the magnetic-field dependence of  $T_1$ .

We finally comment on the generality of our observation. We focused in our analysis on the RHC without magnetic field, or in the fermionic language to a half-filled band. With introducing the field in the XX chain ( $\Delta = 0$ ) the relevant NI-fermion states become even more localized and  $\text{CDF}(s)$  remains  $T$  independent at low- $T$ . Also, our qualitative conclusions on the RHC do not change by adding finite field or



changing  $S_{\text{tot}}^z$  or even reducing  $\Delta < 1$  provided that  $\Delta > 0$  (see Supplement [20]).

We would like to thank M. Klanjšek for useful discussions. This research was supported by the RTN-LOTHERM project and the Slovenian Agency grant No. P1-0044.

- 
- [1] S.-k. Ma, C. Dasgupta, and C.-k. Hu, Phys. Rev. Lett. **43**, 1434 (1979).
  - [2] C. Dasgupta and S.-k. Ma, Phys. Rev. B **22**, 1305 (1980).
  - [3] D. S. Fisher, Phys. Rev. B **50**, 3799 (1994).
  - [4] J. E. Hirsch, Phys. Rev. B **22**, 5355 (1980).
  - [5] A. Zheludev, T. Masuda, G. Dhalenne, A. Revcolevschi, C. Frost, and T. Perring, Phys. Rev. B **75**, 054409 (2007).
  - [6] T. Shiroka, F. Casola, V. Glazkov, A. Zheludev, K. Prša, H.-R. Ott, and J. Mesot, Phys. Rev. Lett. **106**, 137202 (2011).
  - [7] F. Casola, T. Shiroka, V. Glazkov, A. Feiguin, G. Dhalenne, A. Revcolevschi, A. Zheludev, H.-R. Ott, and J. Mesot, Phys. Rev. B **86**, 165111 (2012).
  - [8] E. Westerberg, A. Furusaki, M. Sigrist, and P. A. Lee, Phys. Rev. B **55**, 12578 (1997).
  - [9] O. Motrunich, K. Damle, and D. A. Huse, Phys. Rev. B **63**, 134424 (2001).
  - [10] L. N. Bulaevskii, Zh. Eksp. Teor. Fiz. **62**, 725 (1972).
  - [11] G. Theodorou and M. H. Cohen, Phys. Rev. B **13**, 4597 (1976).
  - [12] T. P. Eggarter and R. Riedinger, Phys. Rev. B **18**, 569 (1978).
  - [13] J. Kokalj and P. Prelovšek, Phys. Rev. B **80**, 205117 (2009).
  - [14] A. W. Sandvik, Phys. Rev. B **52**, R9831 (1995).
  - [15] For a recent review, see P. Prelovšek and J. Bonča, in *Strongly Correlated Systems - Numerical Methods*, edited by A. Avella and F. Mancini (Springer Series in Solid-State Sciences 176, Berlin, 2013), pp. 1–29.
  - [16] S. R. White, Phys. Rev. Lett. **69**, 2863 (1992).
  - [17] U. Schollwöck, Rev. Mod. Phys. **77**, 259 (2005).
  - [18] J. Jaklič and P. Prelovšek, Adv. Phys. **49**, 1 (2000).
  - [19] J. Kokalj and P. Prelovšek, Phys. Rev. B **82**, 060406(R) (2010).
  - [20] See Supplementary material for more details.
  - [21] F. Naef, X. Wang, X. Zotos, and W. von der Linden, Phys. Rev. B **60**, 359 (1999).
  - [22] H. Mori, Prog. Theor. Phys. **34**, 399 (1965).
  - [23] J. Oitmaa, M. Plischke, and T. A. Winchester, Phys. Rev. B **29**, 1321 (1984).
  - [24] T. N. Tommet and D. L. Huber, Phys. Rev. B **11**, 1971 (1975).
  - [25] O. A. Starykh, A. W. Sandvik, and R. R. P. Singh, Phys. Rev. B **55**, 14953 (1997).
  - [26] J. Sirker, R. G. Pereira, and I. Affleck, Phys. Rev. Lett. **103**, 216602 (2009).

## I. NUMERICAL METHOD

In this section we present in more detail the numerical method, finite-temperature dynamical DMRG (FTD-DMRG). The method is a generalization of a zero temperature ( $T = 0$ ) DMRG [S1, S2], with targeting of the ground state or ground state density matrix  $\rho_0 = |0\rangle\langle 0|$  generalized to targeting of the finite- $T$  density matrix  $\rho^\beta = \frac{1}{Z} \sum_n |n\rangle e^{-\beta H} \langle n|$ , [S3–S5]. Similar generalization is applied to targeting of the operator on the ground state. From such targets, generalized to finite- $T$ , the reduced density matrix is calculated and then truncated in the standard DMRG like manner for basis optimization. All quantities, that need to be evaluated at finite- $T$ , are calculated with the use of finite-temperature Lanczos method (FTLM) [S5, S6], which in FTD-DMRG replaces  $T = 0$  Lanczos method used in standard DMRG method.

The method is most efficient at low- $T$  and for low frequencies, where basis can be efficiently truncated and only small portion ( $M$  basis states) of the whole basis for block can be kept. In this regime large system sizes can be reached. The truncation error becomes larger at higher- $T$ , and one needs to either use larger  $M$ , or reduce system size, which is legitimate approach, since finite size effects are smaller at higher- $T$  due to reduced correlation lengths.

We typically keep  $M \sim 200$  basis states in the DMRG block and use systems with length  $L \sim 80$  at low  $T < J/2$ , while for  $T > J/2$  smaller systems are employed down to  $L \sim 20$ , for which full basis can be used. We stress that randomness of  $J_i$  reduces the truncation error since some larger values of  $J_i$  induce strong tension for formation of a local singlet and therefore in turn reduces the entanglement on larger distances. Also the local operator, acting on the middle of the chain, where the local one site basis is not truncated, helps in this respect.

The quenched random  $J_i$  are introduced into the DMRG procedure at the beginning of *finite* algorithm. *Infinite* algorithm is preformed for homogeneous system  $J_i = J$  and the randomness of  $J_i$  is introduced in the first sweep (see Fig. S1 for schematic presentation). In this way the preparation of the basis in the *infinite* algorithm is performed just once and for all realizations of  $J_i$ -s, while larger number of sweeps (usually  $\sim 5$ ) is needed to converge the basis within the *finite* algorithm for random  $J_i$ . After *finite* algorithm local dynamical spin structure factor  $S_{nn}(\omega)$  at desired  $T$  is calculated for the site in the middle of the chain within *measurements* part of DMRG procedure.

Any spectra on finite system consists of separate  $\delta$ -peaks, which we broaden by changing them into Gaussian with small broadening  $\delta = 0.05$  and in this way obtain a smooth spectra.

Since NMR relaxation rate is related to  $S_{nn}(\omega \rightarrow 0)$ , we are interested in the limit  $\omega \rightarrow 0$ , which should be contrasted with the static (d.c.)  $S_{nn}(\omega = 0)$ . The latter is given by diagonal elements, which in a system with random  $J_i$  appear due to nontrivial overlap of  $S_n^z$  with the conserved total spin  $S_{\text{tot}}^z$ , explicitly  $\langle S_n^z S_{\text{tot}}^z \rangle \neq 0$ . In order to avoid the problem

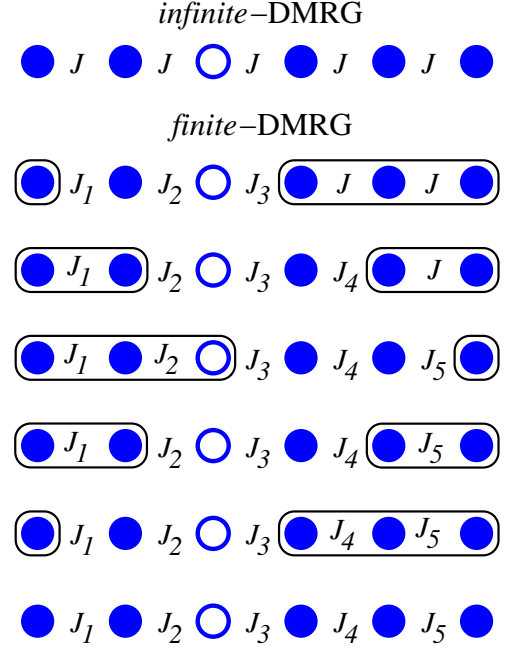


Figure S1. (Color online) Schematic ( $L = 6$ ) representation of the beginning of the sweeping method in *finite*-DMRG algorithm, in which randomness is introduced. Open circle represents site of a local operator used to calculated local dynamical spin structure factor in the *measurement* part of the DMRG method.

of diagonal elements and keeping  $\omega \neq 0$  we perform the evaluation of  $S_{nn}(\omega \rightarrow 0)$  in the magnetisation sector  $S_{\text{tot}}^z = 0$ , which in terms of spinless fermions corresponds to the canonical ensemble. In the thermodynamic limit, both canonical and grand canonical calculations should give the same result.

Diagonal elements are however essential when evaluating static uniform susceptibility  $\chi^0(T) = \langle (S_{\text{tot}}^z)^2 \rangle / (LT)$ , which we show in Fig. S2. It has been argued [S7–S9], that in 1D random Heisenberg chain the density of low lying excitation is strongly increased, which is observed in diverging  $\chi^0(T)$  for  $T \rightarrow 0$ . Our numerical results show similar behavior (see Fig. S2), which agrees also with experiment [S10, S11].

Increased number of low-lying excitations (see Fig. S2) also reduces the finite size effect, since, e.g., finite size gap is reduced, and in this way also the temperature  $T_{\text{fs}}$ , below which the finite size effects become important. Therefore, smaller  $T$  can be numerically reached in a random system.

## II. HIGH- $T$ EXPANSION

The local spin correlation function can be related to the (local) dynamical spin susceptibility by relation

$$S_{nn}(\omega) [1 - \exp(-\beta\omega)] = \chi''_{nn}(\omega), \quad (\text{S1})$$

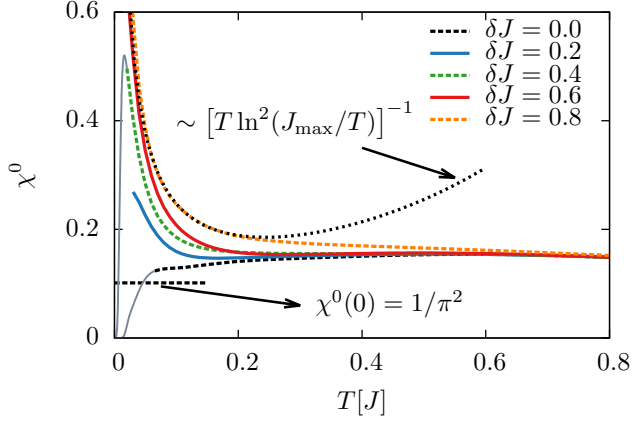


Figure S2. (Color online) Static spin susceptibility  $\chi^0(T)$  vs. temperature  $T$  for various randomness  $\delta J$ . For random system ( $\delta J \neq 0$ )  $\chi^0(T)$  is strongly increased at low- $T$  and agrees with the random singlet [S7] prediction (black dotted line). Sudden drop of  $\chi^0(T)$  at low- $T$  shown for  $\delta J = 0$  and  $\delta J = 0.4$  represents opening of finite-size gap, which is strongly reduced in the random (shown for  $\delta J = 0.4$ ) system. Results are obtained with the finite-temperature Lanczos method [S5, S6] on  $L = 24$  sites.

with

$$\chi_{nn}(\omega) = i \int_0^\infty dt e^{i\omega t} \langle [S_n^z(t), S_n^z(0)] \rangle. \quad (\text{S2})$$

Taking the high- $T$  limit ( $\beta \rightarrow 0$ ) of Eq. (S1) one gets  $\beta S_{nn}(\omega) = \chi''_{nn}(\omega)/\omega$ , which is so-called relaxation function - symmetric with respect to  $\omega = 0$ , non-negative function. Note that due to symmetric form of relaxation function all odd frequency moments,  $m_{ln}$ , are equal to zero.

The local spin correlation function can be expressed by the Mori's continued fraction representation [S12]:

$$\hat{S}_{nn}(z = i\omega) = \frac{\delta_{0n}}{z + \frac{\delta_{1n}}{z + \frac{\delta_{2n}}{z + \dots}}}, \quad (\text{S3})$$

where coefficient  $\delta_{ln}$  are cumulants of  $S_{nn}(\omega)$ , i.e.  $\delta_{0n} = m_{0n}$ ,  $\delta_{1n} = m_{2n}/m_{0n}$ ,  $\delta_{2n} = m_{4n}/m_{2n} - m_{2n}^2/m_{0n}^2$ .  $m_{ln}$  are frequency moments of the local spectra,  $m_{ln} = \int d\omega \omega^l S_{nn}(\omega)$ .

For  $l > 3$  we chose a truncation  $\zeta_n = \delta_{3n}/(z + \dots)$ , which assumes [S13, S14] a Gaussian-like decay of correlation function, i.e.  $\zeta_n = \sqrt{2/\pi}(\delta_{1n} + \delta_{2n})/\delta_{2n}^{3/2}$ . The  $S_{nn}(\omega)$  can be recovered from Eq. (S3) by the relation  $S_{nn}(\omega) = \text{Re}[\hat{S}_{nn}(z = i\omega)]/\pi$ , leading to

$$S_{nn}(\omega) = \frac{1}{\pi} \frac{\zeta_n \delta_{0n} \delta_{1n} \delta_{2n}}{[\omega \zeta_n (\omega^2 - \delta_{1n} - \delta_{2n})]^2 + (\omega^2 - \delta_{1n})^2}, \quad (\text{S4})$$

Note that Eq. (S4) gives the first three nonzero ( $l = 0, 2, 4$ ) frequency moments  $m_{ln}$  correctly, independent of a choice of  $\zeta_n$ .

Frequency moments  $m_{ln}$  of  $S_{nn}(\omega)$  can be evaluated analytically for  $T = \infty$ , e.g.,  $m_{0n} = \langle S_n^z S_n^z \rangle$ ,  $m_{2n} = \langle [H, S_n^z][H, S_n^z] \rangle$ , etc. For zero magnetisation,  $S_{\text{tot}}^z = |L_\uparrow - L_\downarrow|/2L = 0$ , where  $L_\uparrow$  ( $L_\downarrow$ ) is number of up (down) spins, the first three nonzero moments of the order of  $\mathcal{O}(\beta)$  are:

$$\begin{aligned} m_{0n} &= \frac{1}{4}, & m_{2n} &= \frac{J_{n-1}^2 + J_n^2}{8}, \\ m_{4n} &= \frac{1 + \Delta^2}{32} (J_{n-2}^2 J_{n-1}^2 + J_n^2 J_{n+1}^2) \\ &+ \frac{3 + 2\Delta^2}{32} (J_{n-1}^4 + J_n^4) + \frac{7 + 2\Delta^2}{32} J_{n-1}^2 J_n^2. \end{aligned} \quad (\text{S5})$$

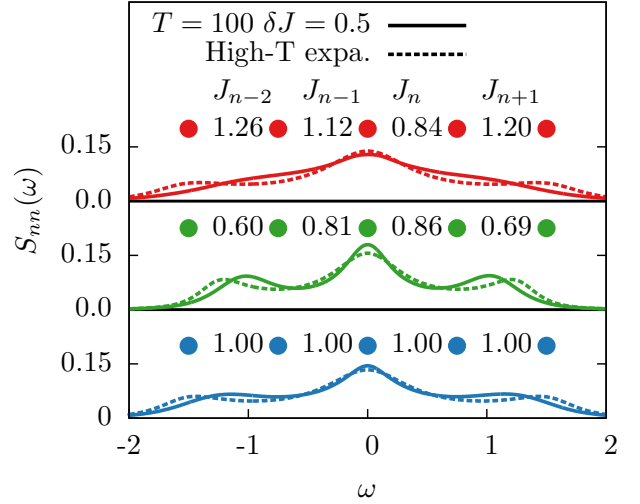


Figure S3. (Color online) Comparison of  $S_{nn}(\omega)$  between analytical high- $T$  expansion result and numerical FTD-DMRG result ( $L = 20$ ,  $T = 100$ , full basis) for three realization of  $J_i$ .

In Fig. S3 we present comparison of high- $T$  expansion result and FTD-DMRG result ( $L = 20$ ,  $T = 100$ , full basis) for  $S_{nn}(\omega)$  and three realizations of  $J_i$ . One can see that the agreement is good for actual finite size system. It should be, however, noted that  $q \rightarrow 0$  contribution (leading to finite size corrections) can become essential for  $T \gg J$  [S15].

As a final remark of this section we comment on the probability distribution function (PDF) of  $s = S_{nn}(\omega \rightarrow 0)$  presented in Fig. 2 in the main text. Assuming the uniform distribution of  $J_i$ ,  $i = n - 2, \dots, n + 1$  the PDF( $s$ ) can be generated from expression

$$s = S_{nn}(\omega \rightarrow 0) = \frac{1}{\sqrt{8\pi^3}} \frac{\delta_{1n} + \delta_{2n}}{\delta_{1n} \delta_{2n}^{1/2}}. \quad (\text{S6})$$

The PDF's presented in Fig. 2 (main text) were obtained from  $N_r = 10^6$  realizations of  $J_i$ .

### III. FINITE MAGNETIC FIELD AND $\Delta = 0.5$

In Fig. S4 we show that our main conclusions stay valid also in a more general case, such as for  $\Delta = 0.5 < 1$  and

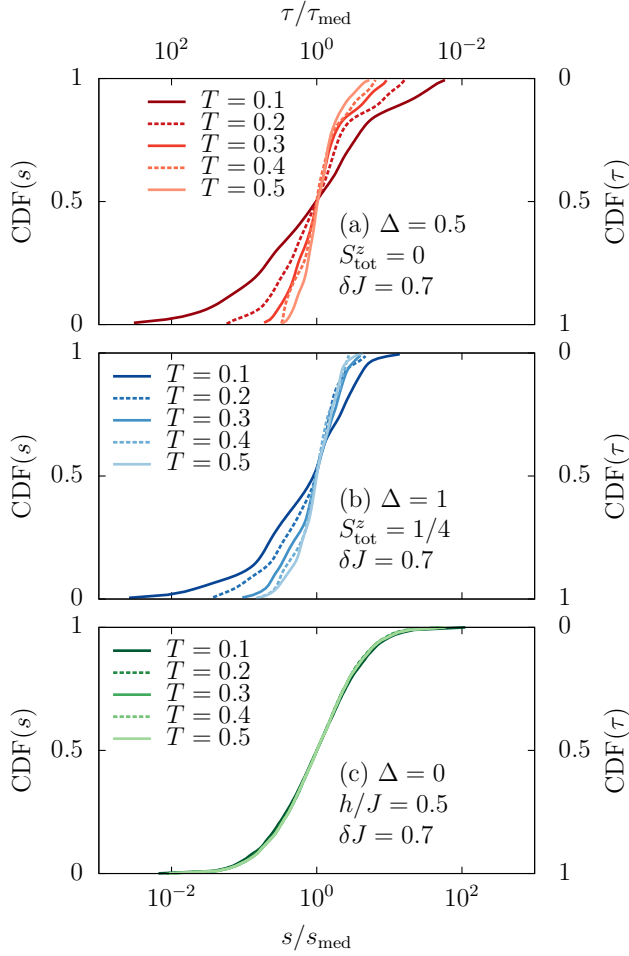


Figure S4. (Color online) Cumulative distribution function of relaxation rates  $s$  and times  $\tau = 1/s$ . Shown are FTD-DMRG results for various  $T \leq 0.5$  and: (a) for  $\Delta = 0.5$ ,  $S_{\text{tot}}^z = 0$  and  $\delta J = 0.7$ , (b) for  $\Delta = 1$ ,  $S_{\text{tot}}^z = 1/4$  and  $\delta J = 0.7$ , while (c) are diagonalization results for  $\Delta = 0$ ,  $\delta J = 0.7$  and  $h/J = 0.5$ .

for finite magnetisation ( $S_{\text{tot}}^z = 1/4$ ), where considerable  $T$  dependence of distribution with large spread is observed. In the last panel of Fig. S4 we show that the distribution for noninteracting case (XX model) stays  $T$  independent even in a finite magnetic field  $h$  or for finite magnetisation.

- 
- [S1] S. R. White, Phys. Rev. Lett. **69**, 2863 (1992).
  - [S2] U. Schollwöck, Rev. Mod. Phys. **77**, 259 (2005).
  - [S3] J. Kokalj and P. Prelovšek, Phys. Rev. B **80**, 205117 (2009).
  - [S4] J. Kokalj and P. Prelovšek, Phys. Rev. B **82**, 060406(R) (2010).
  - [S5] For a recent review, see P. Prelovšek and J. Bonča, in *Strongly Correlated Systems - Numerical Methods*, edited by A. Avella and F. Mancini (Springer Series in Solid-State Sciences 176, Berlin, 2013), pp. 1–29.
  - [S6] J. Jaklič and P. Prelovšek, Adv. Phys. **49**, 1 (2000).
  - [S7] D. Fisher, Phys. Rev. B **50**, 3799 (1994).
  - [S8] J. E. Hirsch, Phys. Rev. B **22**, 5355 (1980).
  - [S9] A. Zheludev, T. Masuda, G. Dhalenne, A. Revcolevschi, C. Frost, and T. Perring, Phys. Rev. B **75**, 054409 (2007).
  - [S10] T. Shiroka, F. Casola, V. Glazkov, A. Zheludev, K. Prša, H.–R. Ott, and J. Mesot, Phys. Rev. Lett. **106**, 137202 (2011).
  - [S11] T. Masuda, A. Zheludev, K. Uchinokura, J.-H. Chung, and S. Park, Phys. Rev. Lett. **93**, 077206 (2004).
  - [S12] H. Mori, Prog. Theor. Phys. **34**, 399 (1965).
  - [S13] T. N. Tommet and D. L. Huber, Phys. Rev. B **11**, 1971 (1975).
  - [S14] J. Oitmaa, M. Plischke, and T. A. Winchester, Phys. Rev. B **29**, 1321 (1984).
  - [S15] O. A. Starykh, A. W. Sandvik, and R. R. P. Singh, Phys. Rev. B **55**, 14953 (1997).